

Electronic Supplementary Information for

Carving Growing Nanocrystals: Coupling Seed-Mediated Growth with Oxidative Etching

*Esteban Villarreal, Guangfang Grace Li, and Hui Wang**

*Department of Chemistry and Biochemistry, University of South Carolina, Columbia, South Carolina
29208, United States*

** To whom correspondence should be addressed.*

Email: wang344@mailbox.sc.edu; Phone: 1-803-777-2203; Fax: 1-803-777-9521.

S1. Experimental Details

S1.1. Chemicals and Materials

All reagents were used as received without further purification. Gold(III) chloride trihydrate ($\text{HAuCl}_4 \cdot 3\text{H}_2\text{O}$, ACS grade) was purchased from J.T. Baker. Sodium borohydride (NaBH_4 , 99%), hydrochloric acid (HCl, 37%), and L-ascorbic acid (AA, 99.5%) were obtained from Sigma-Aldrich. Cetyltrimethylammonium chloride (CTAC, 96%) and silver nitrate (AgNO_3 , 99.9995% metal basis) were obtained from Alfa Aesar. Ultrapure water (18.2 M Ω resistivity, Barnstead EasyPure II 7138) was used for all experiments.

S1.2. Synthesis of Au Seeds

Colloidal Au seeds (~ 4 nm in diameter) were synthesized by reducing HAuCl_4 with NaBH_4 in the presence of CTAC following a previously reported protocol.¹⁻³ Briefly, 0.25 mL of HAuCl_4 (10 mM) was introduced into an aqueous solution of CTAC (10 mL, 100 mM) under magnetic stir. Then 0.30 mL of ice cold, freshly prepared NaBH_4 (10 mM) was quickly added to the solution containing both CTAC and HAuCl_4 . The mixture solution was stirred for 1 min, then left undisturbed for 2 h at room temperature under ambient air, and finally diluted 1000-fold with 100 mM CTAC. The diluted seed colloids were used for the subsequent seed-mediated growth of various nanostructures.

S1.3. Seed-Mediated Nanocrystal Growth

The shape-controlled nanocrystal growth was initiated by introducing 40 μL of the diluted Au seeds into an aqueous growth solution containing HAuCl_4 , AA, HCl, AgNO_3 , and CTAC. The total volume of the growth solution was 10 mL and the concentrations of CTAC and HAuCl_4 were kept at 100 mM and 500 μM , respectively. The concentrations of HCl, AA, and AgNO_3 were systematically varied to tune the rate of the nanocrystal growth relative to that of oxidative etching, based on which the shapes and surface topography of the resulting nanocrystals were fine-tailored. Upon the addition of seeds, the reactants were gently mixed for 30 s and then left undisturbed at room temperature under ambient air for various reaction times. To control the concentration of oxygen dissolved in the growth solutions, the solutions containing the reactants were purged with N_2 or O_2 for 1 h before mixing and the reaction mixtures were then kept under N_2 or O_2 atmospheres throughout the reaction processes. The as-obtained nanoparticles were washed with water 3 times through centrifugation/redispersion cycles, and finally redispersed in water.

S1.4. Structural Characterizations

The structures of the nanoparticles were characterized by scanning electron microscopy (SEM) using a Zeiss Ultraplus thermal field emission scanning electron microscope. The samples for SEM measurements were dispersed in water and drop-dried on silicon wafers. An energy dispersive spectroscopy (EDS) elemental analysis unit attached to the microscope was used to map the spatial distribution of Au and Ag elements in each nanoparticle. The bulk Ag:Au atomic ratios of various samples were quantified based on the relative areas of the Ag $\text{L}\alpha$ and Au $\text{L}\alpha$ peaks in the spectra. The Au seeds were imaged by transmission electron microscopy (TEM) using a Hitachi HT7800 transmission electron microscope, which was operated at an accelerating voltage of 120 kV. XPS measurements were carried out using a Krato AXIS Ultra DLD XPS system equipped with a monochromatic Al $\text{K}\alpha$ source. The samples for XPS measurements were all freshly prepared and dried in vacuum before being loaded into the XPS chambers. The surface Ag:Au atomic ratios of various samples were quantified based on the relative areas of the Ag 3d and Au 4f peaks in the spectra. The sample penetration depth of the XPS measurements under the current experimental conditions was calibrated to be ~ 1 nm,⁴ roughly corresponding to 5 atomic layers from the outer surface of the nanoparticles. Therefore, the formation of a saturated monolayer coverage of Ag UPD adatoms on the Au nanoparticles would ideally result in an Ag/Au

atomic ratio of ~ 0.25 . The standard deviations of the Ag: Au atomic ratios quantified by EDS and XPS were obtained from 3 samples synthesized under identical conditions and shown as the error bars in Figure 1H, Figure S6, and Figure S11. The optical extinction spectra of the nanoparticles were measured on aqueous colloidal suspensions at room temperature using a Beckman Coulter Du 640 spectrophotometer. The total amounts of gold and silver remaining in the supernatant at various reaction times were quantified using a Finnigan ELEMENT XR double focusing magnetic sector field inductively coupled plasma-mass spectrometer (SF-ICP-MS) after separating the nanocrystals from the growth solutions.

S2. Additional Discussion of the Temporal Evolution of Optical Extinction Spectra

The surface-roughened quasi-spherical nanoparticles (SRQSNPs), surface-textured concave nanocubes (STCNCs), and excavated cuboctahedral nanoparticles (ECONPs) all exhibited plasmonic characteristics sensitively dependent upon their sizes, shapes, and surface topography. Therefore, the structural evolution of the nanocrystals could be monitored *in situ* using optical extinction spectroscopy without separating the nanocrystals from their growth solutions. The plasmon resonance band of the Au-Ag alloy SRQSNPs progressively red-shifted and broadened as the particle size increased (Figure S8A), in line with previous observations on the surface-roughened Au nanoparticles.⁵ When the SRQSNPs became larger than ~ 150 nm, a spectral feature corresponding to the quadrupole resonance emerged around 650 nm in addition to the dipole resonance due to phase retardation effects.⁶⁻⁹ For the STCNCs, the surface indentation led to spectral redshift of the plasmon resonance, while the nanoscale surface texturing caused significant broadening of the peaks (Figure S8B). During the growth of ECONPs, the plasmon resonance peak first underwent a red-shifting and broadening process due to surface indentation and texturing, and then blue-shifted upon corner truncation at the later stages of the reactions (Figure S8C). Besides the plasmon resonance peaks in the visible and near-infrared, the spectral feature in the wavelength range below 400 nm arose from the interband electronic transitions of Au. Because the intensity of extinction due to interband transitions was qualitatively proportional to the Au mass in the nanocrystals, the rate of the mass increase of growing nanocrystals could be straightforwardly tracked by monitoring the temporal evolution of the optical extinction at 350 nm (Figure S8D), which showed that the nanocrystal growth rates decreased with increase of HCl concentration.

S3. Additional Figures

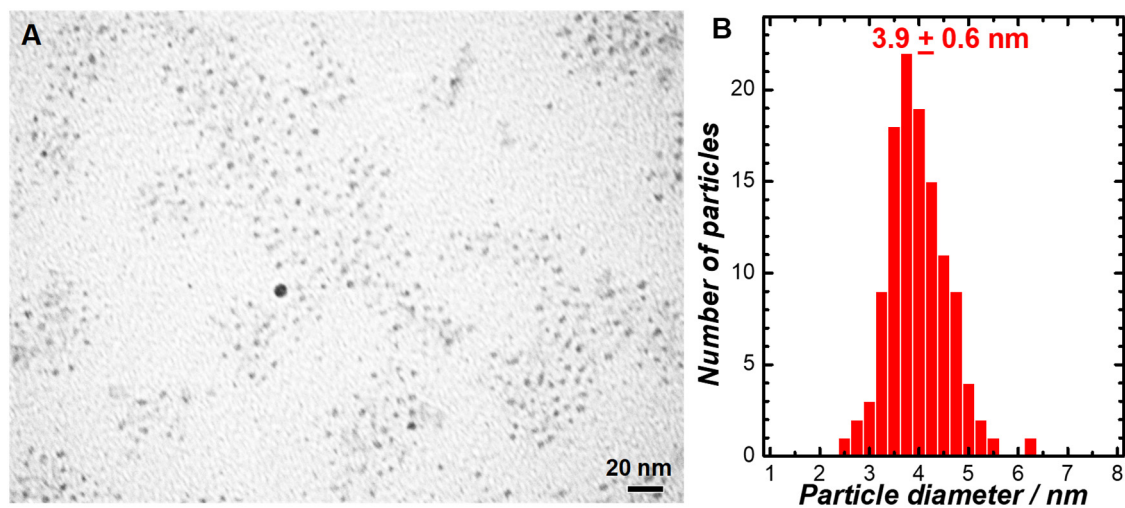


Figure S1. (A) TEM image and (B) size distribution of colloidal Au seeds.

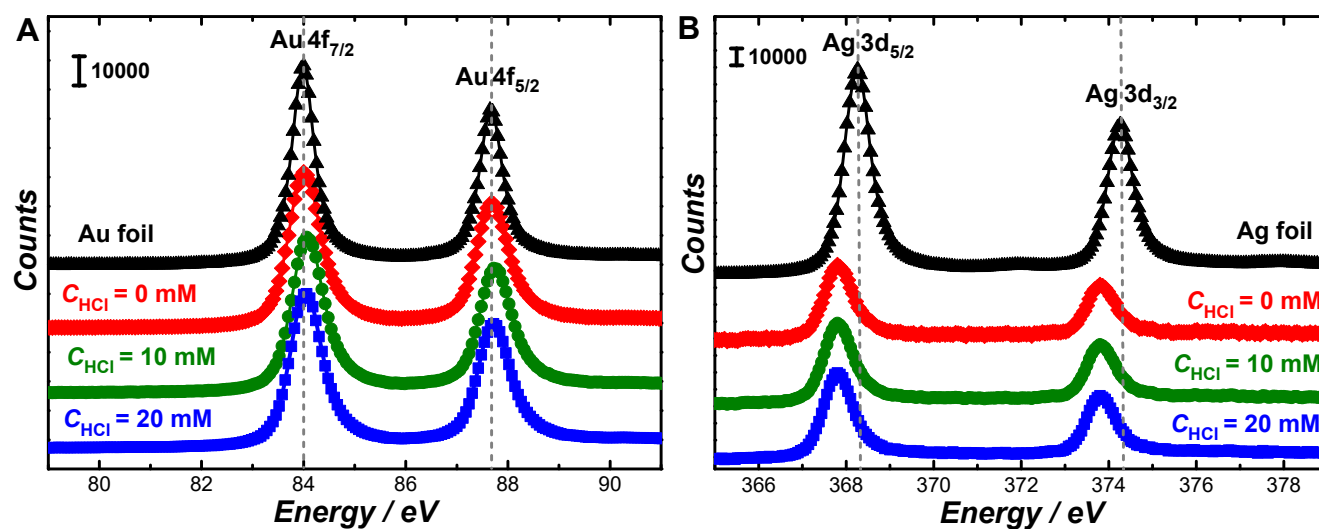


Figure S2. XPS spectra of (A) Au 4f and (B) Ag 3d regions of nanoparticles synthesized after 16 h in 100 mM CTAC, 50 μM AgNO_3 , 500 μM HAuCl_4 , and 1.2 mM AA in the presence of 0, 10, and 20 mM HCl. The spectra of a bulk Au foil and Ag foil were also shown for comparison. The spectra were offset for clarity.

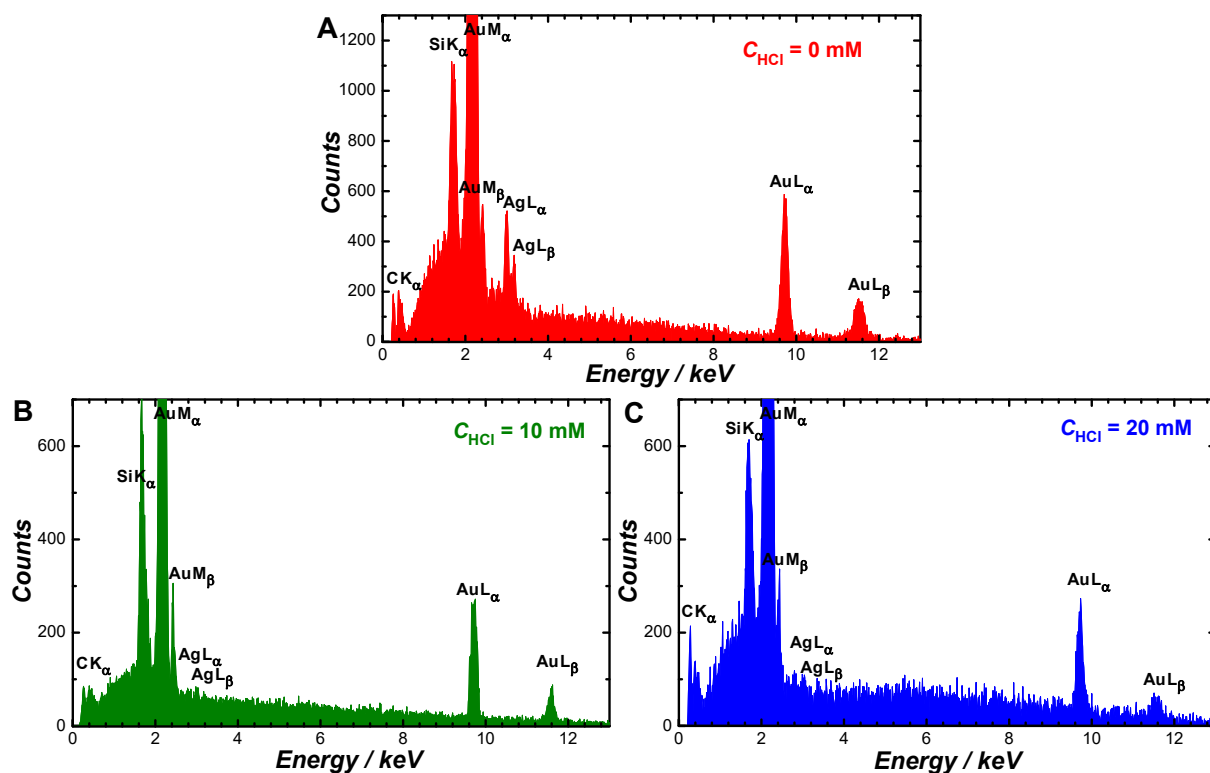


Figure S3. EDS spectra of nanoparticles synthesized after 16 h in 100 mM CTAC, 50 μM AgNO_3 , 500 μM HAuCl_4 , 1.2 mM AA, and (A) 0, (B) 10, and (C) 20 mM HCl. The Si signals were from the Si substrates.

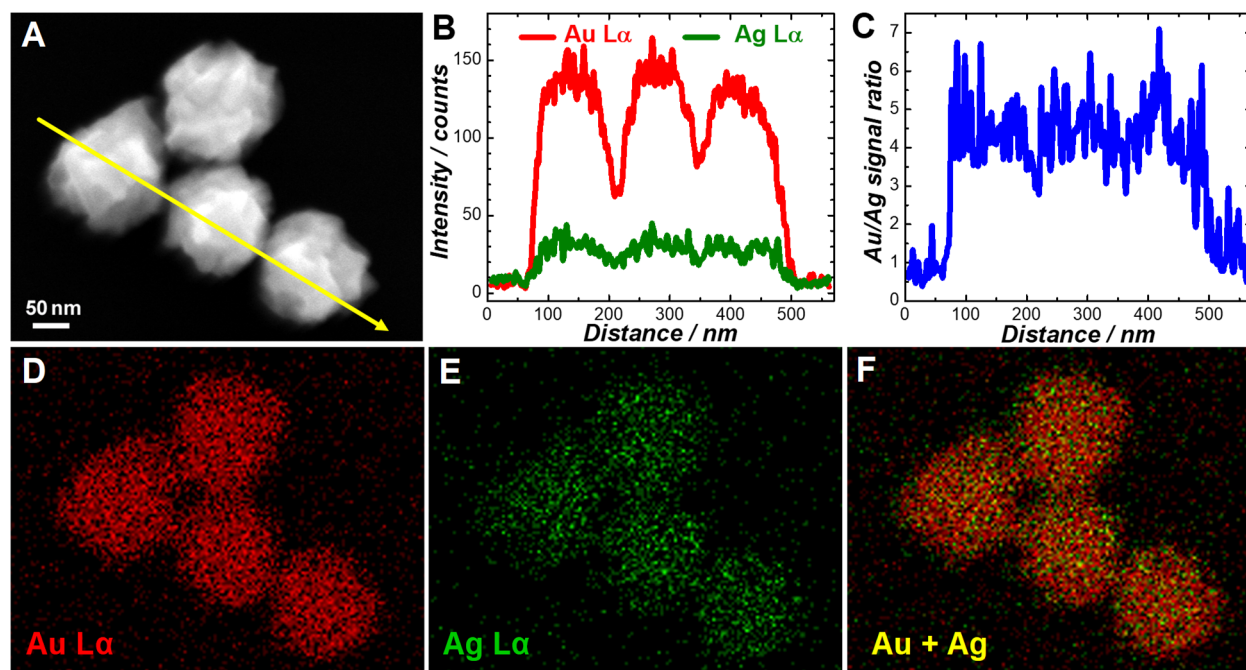


Figure S4. (A) SEM image of Au-Ag alloy surface-textured quasi-spherical nanoparticles synthesized after 16 h in a growth solution containing 100 mM CTAC, 50 μM AgNO_3 , 500 μM HAuCl_4 , and 1.2 mM AA. (B) Line-profiles of EDS intensities of Au L α and Ag L α , and (C) line-profile of Au/Ag signal ratios across the yellow line in panel A. EDS elemental maps of (D) Au, (E) Ag, and (F) overlay of Au + Ag.

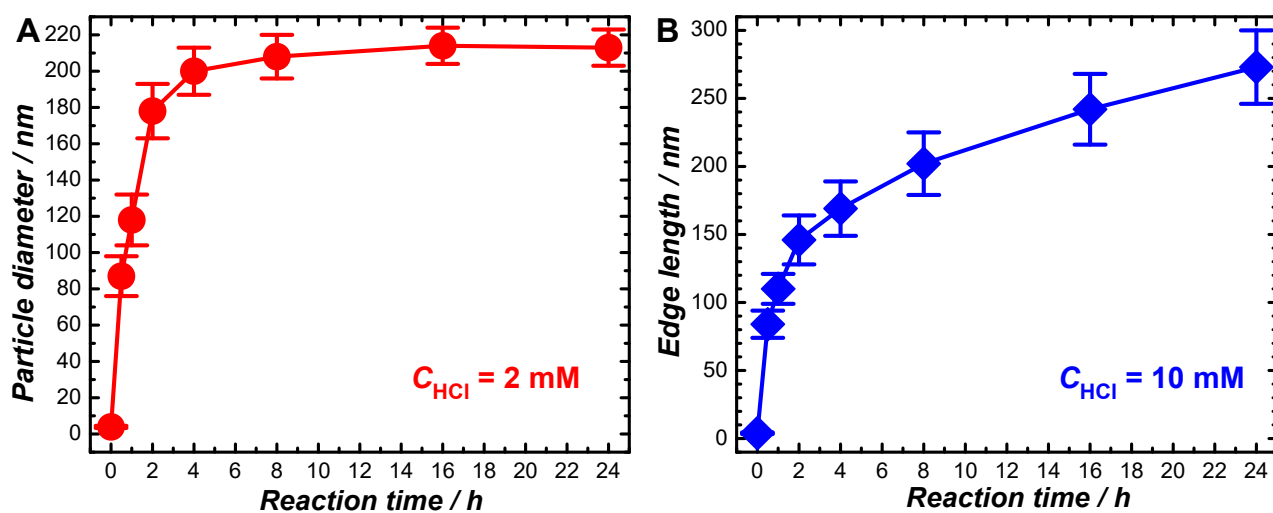


Figure S5. Temporal evolution of particle sizes during the seed-mediated nanocrystal growth in growth solutions containing 100 mM CTAC, 50 μM AgNO_3 , 500 μM HAuCl_4 , 1.2 mM AA, and (A) 2 and (B) 10 mM HCl. The average particle sizes and standard deviations were obtained from 100 particles in the SEM images for each sample. The Au seeds were 3.9 ± 0.6 nm in diameter.

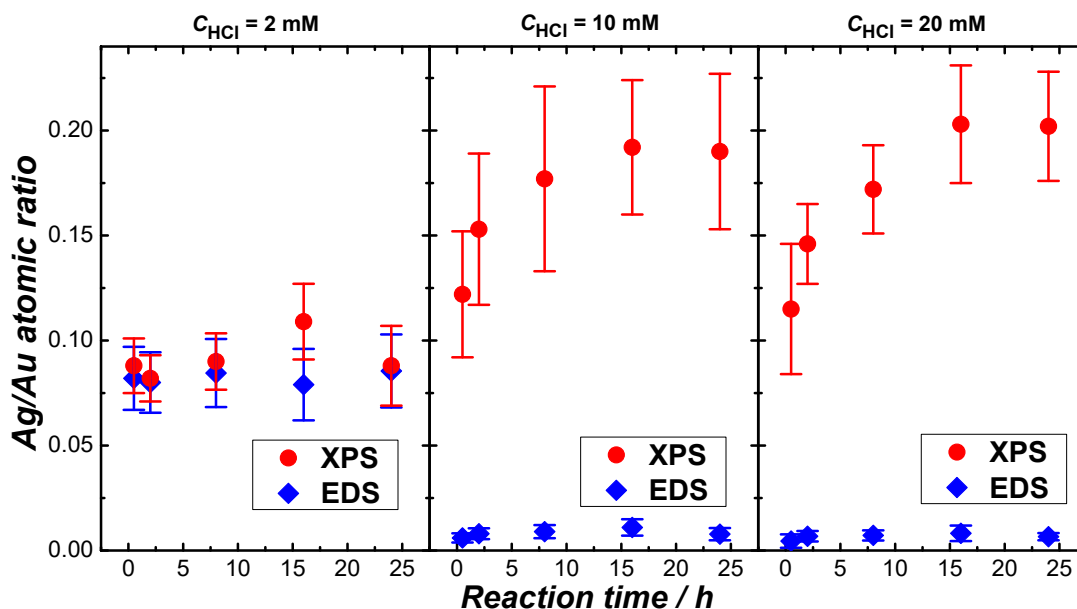


Figure S6. Temporal evolution of surface Ag/Au atomic ratio (quantified by XPS) and bulk Ag/Au atomic ratio (quantified by EDS) during seed-mediated nanocrystal growth in growth solutions containing 100 mM CTAC, 50 μM AgNO_3 , 500 μM HAuCl_4 , 1.2 mM AA, and (left panel) 2, (middle panel) 10, and (right panel) 20 mM HCl. The error bars represent the standard deviations obtained from 3 samples synthesized under identical conditions.

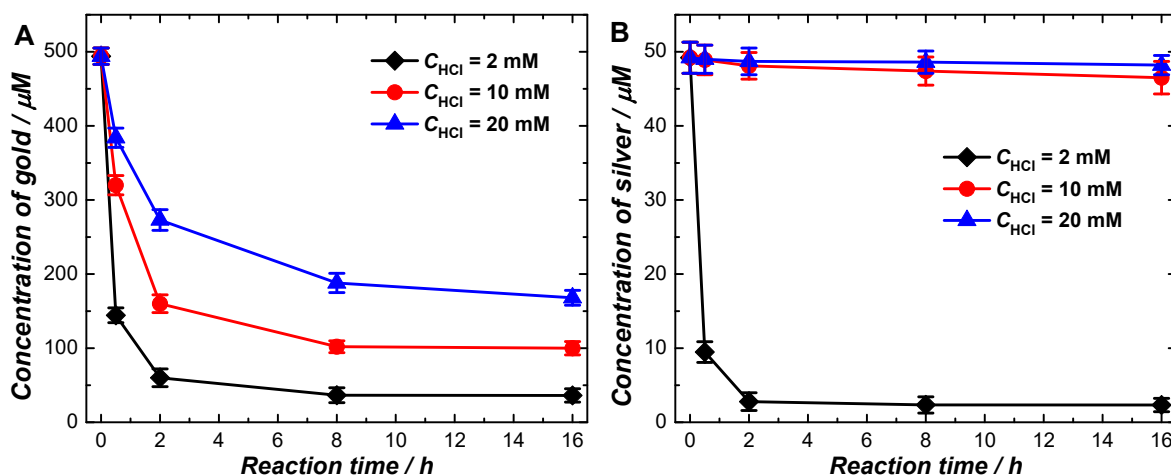


Figure S7. Total amounts of (A) gold and (B) silver remaining in the supernatant at various reaction times quantified by ICP-MS. The growth solutions contained 100 mM CTAC, 50 μM AgNO_3 , 500 μM HAuCl_4 , 1.2 mM AA, and 2, 10, or 20 mM HCl.

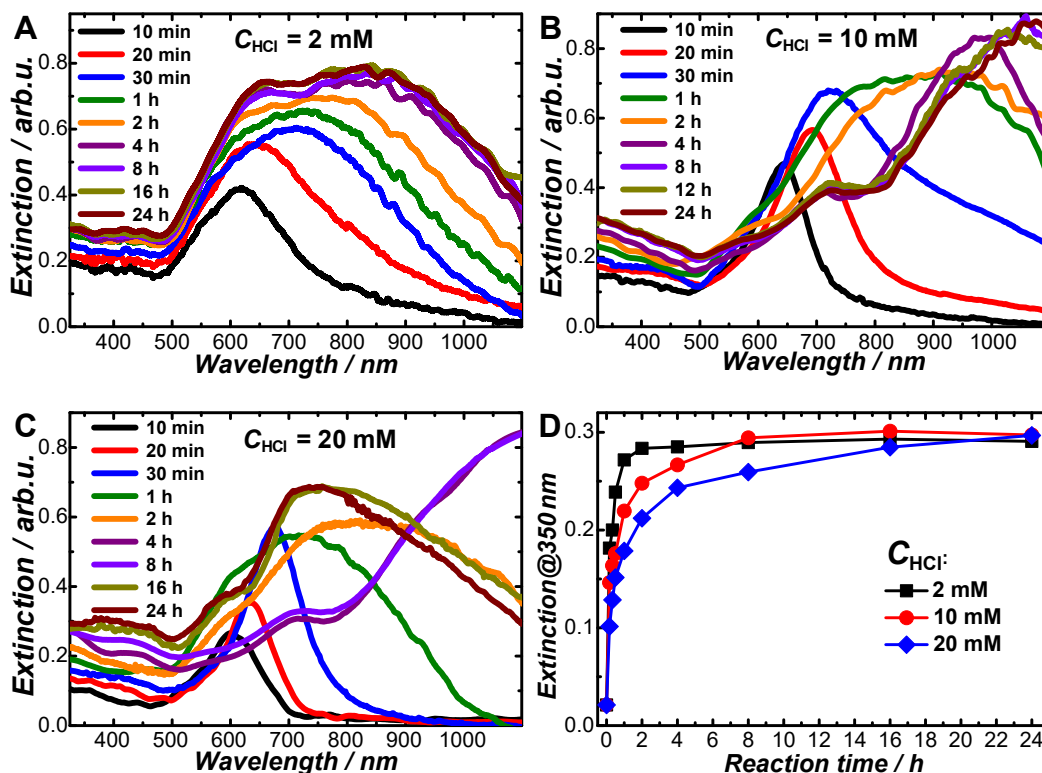


Figure S8. Temporal evolution of optical extinction spectra during nanocrystal growth in 100 mM CTAC, 50 μM AgNO_3 , 500 μM HAuCl_4 , 1.2 mM AA, and (A) 2 mM, (B) 10 mM, and (C) 20 mM HCl. (D) Temporal evolution of optical extinction at 350 nm.

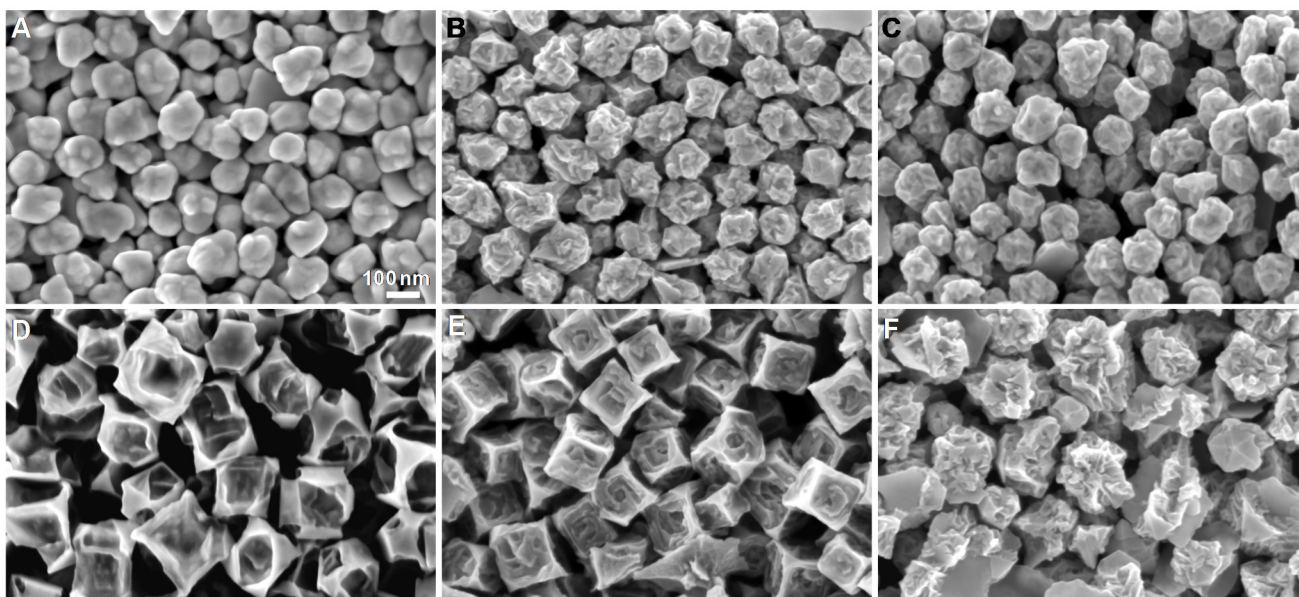


Figure S9. Effects of AA. SEM images of nanoparticles synthesized after 16 h in growth solutions containing 100 mM CTAC, 50 μM AgNO_3 , 500 μM HAuCl_4 , and various concentrations of AA and HCl: (A) 0.5 mM AA, 2 mM HCl; (B) 1 mM AA, 2 mM HCl; (C) 5 mM AA, 2 mM HCl; (D) 1 mM AA, 20 mL HCl; (E) 2.5 mM AA, 20 mL; (F) 5 mM AA, 20 mM HCl. All SEM images share the same scale bar in panel A.

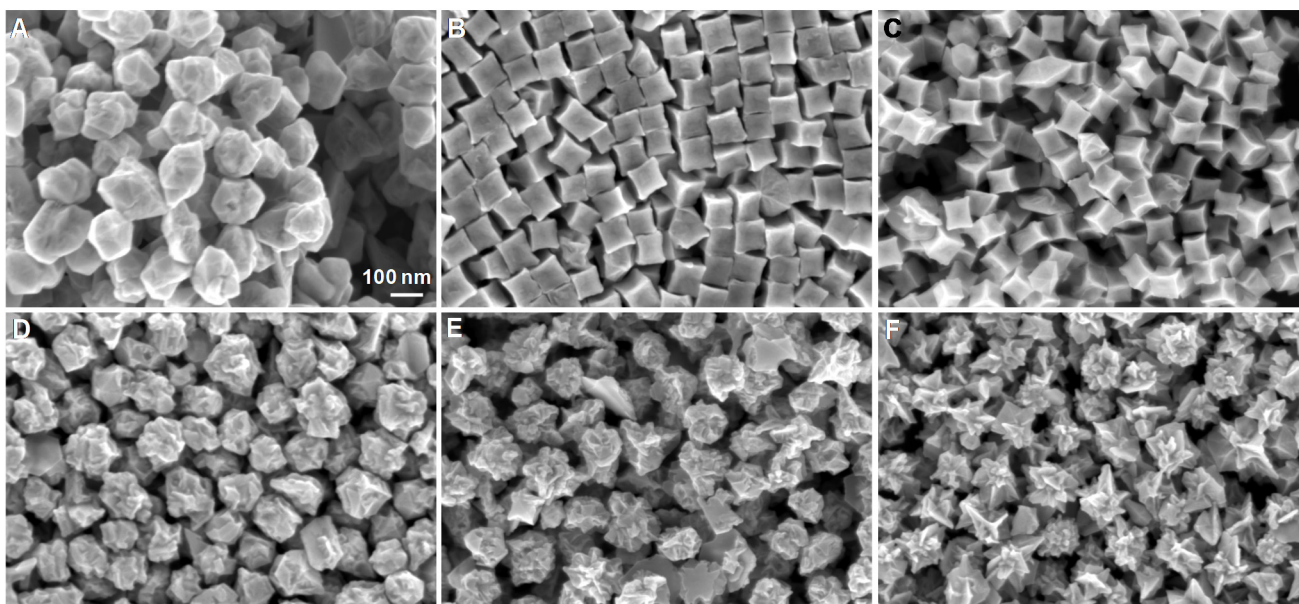


Figure S10. Effects of dissolved oxygen. SEM images of nanoparticles synthesized after 16 h in oxygen-purged growth solutions containing 100 mM CTAC, 50 μM AgNO_3 , 500 μM HAuCl_4 , 1.2 mM AA, and (A) 2, (B) 10, and (C) 20 mM HCl. SEM images of nanoparticles synthesis after 16 h in deoxygenated (purged with N_2) growth solutions containing 100 mM CTAC, 50 μM AgNO_3 , 500 μM HAuCl_4 , 1.2 mM AA, and (D) 2, (E) 10, and (F) 20 mM HCl. All SEM images share the same scale bar in panel A.

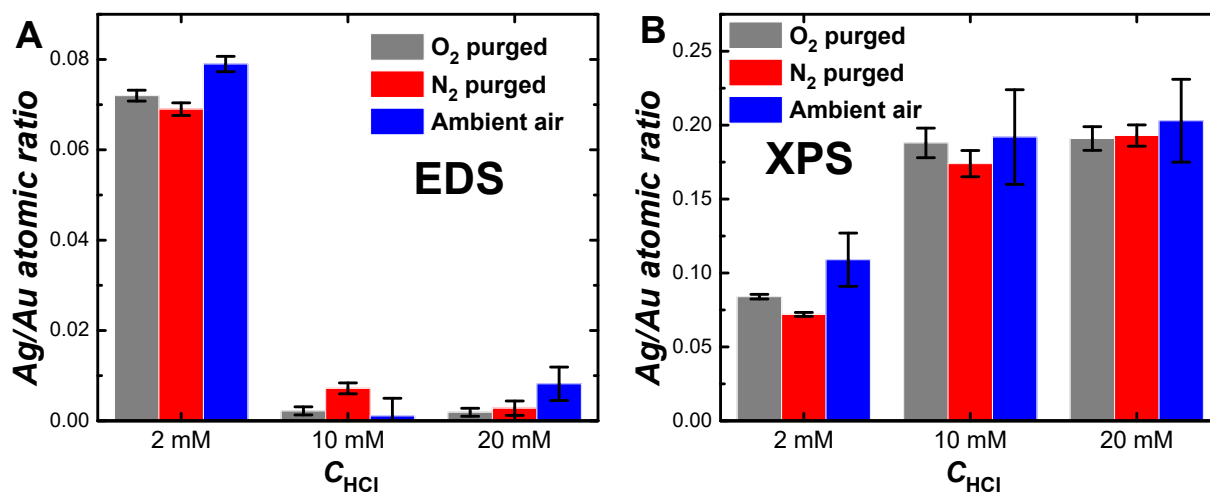


Figure S11. (A) Bulk Ag/Au atomic ratio quantified by EDS and (B) surface Ag/Au atomic ratio quantified by XPS for nanoparticle samples synthesized after 16 h in growth solutions containing 100 mM CTAC, 50 μM AgNO_3 , 500 μM HAuCl_4 , 1.2 mM AA, and 2, 10, and 20 mM HCl. The growth solutions were either exposed to ambient air or purged with O_2 or N_2 . The error bars represent the standard deviations obtained from 3 samples synthesized under identical conditions.

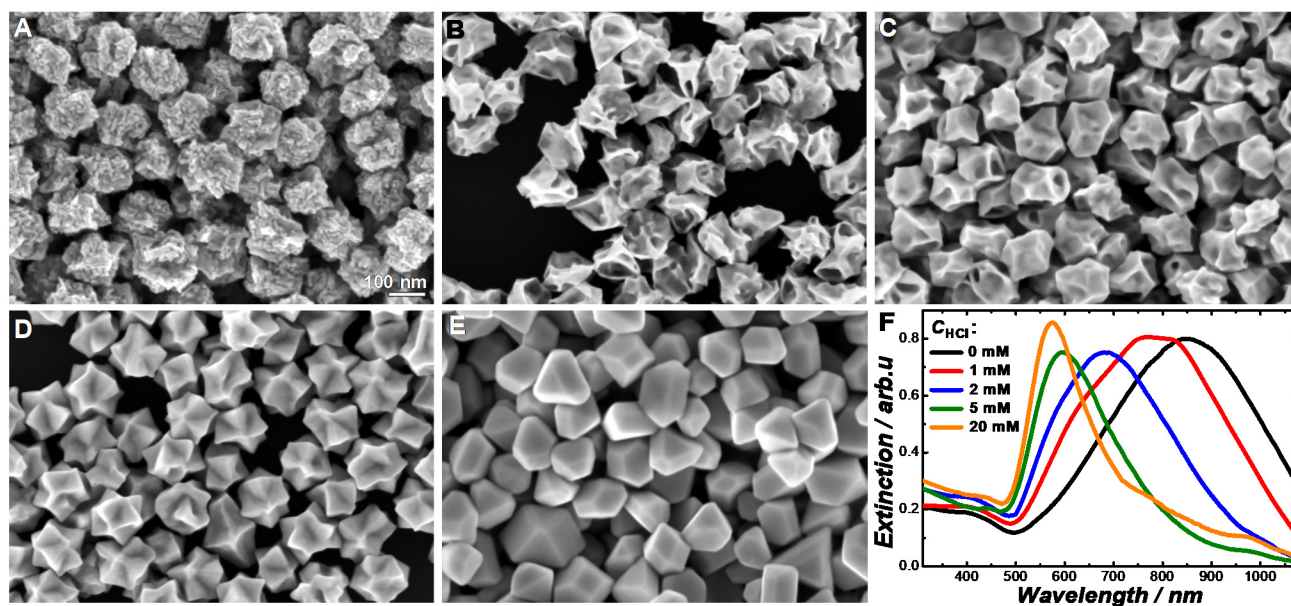


Figure S12. Etching and growth of Au nanoparticles in the absence of AgNO_3 . Au nanoparticles synthesized after 16 h in growth solutions containing 100 mM CTAC, 500 μM HAuCl_4 , 1.2 mM AA, and (A) 0, (B) 1, (C) 2, (D) 5, and (E) 20 mM HCl. All SEM images share the same scale bar in panel A. (F) Optical extinction spectra of colloidal Au nanoparticles synthesized after 16 h in growth solutions containing 100 mM CTAC, 500 μM HAuCl_4 , 1.2 mM AA, and various concentrations of HCl as labeled in the figure.

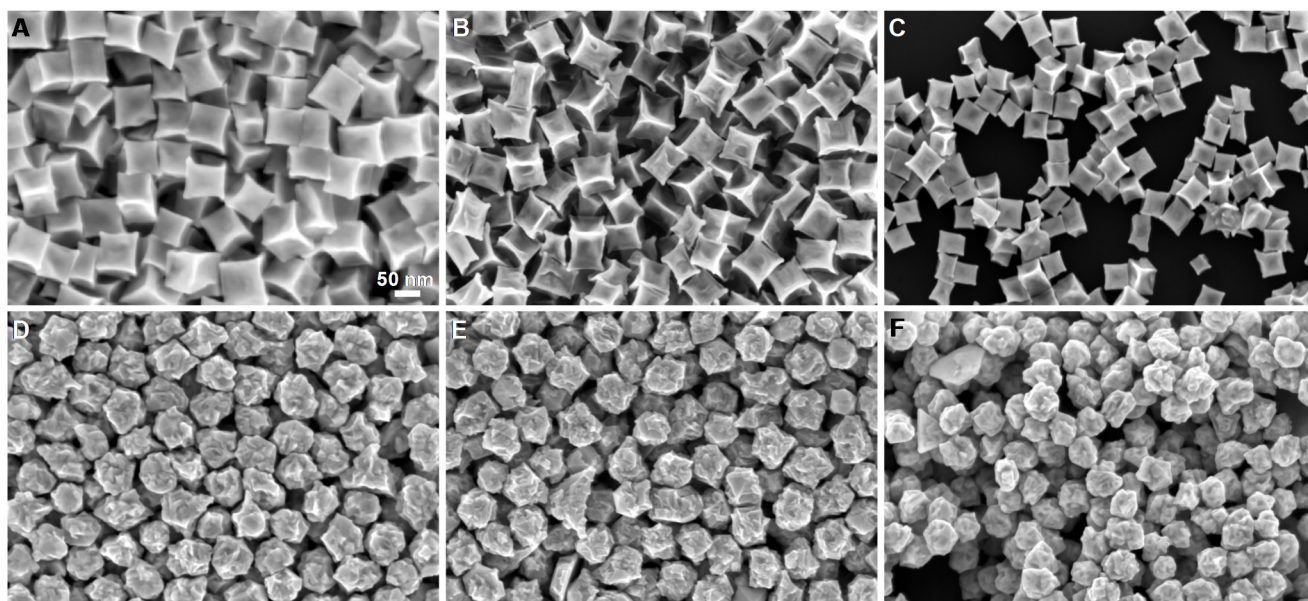


Figure S13. (A) SEM image of nanoparticles synthesized after 1 h in a growth solution containing 100 mM CTAC, 500 μM HAuCl_4 , 50 μM AgNO_3 , 1.2 mM AA, and 10 mM HCl. SEM images of the nanoparticles shown in panel A after post-synthetic etching for 16 h in etching solutions containing 100 mM CTAC and 10 mM HCl (B) in the presence of 50 μM AgNO_3 and (C) in the absence of AgNO_3 . (D) SEM image of nanoparticles synthesized after 1 h in a growth solution containing 100 mM CTAC, 500 μM HAuCl_4 , 50 μM AgNO_3 , 1.2 mM AA, and 2 mM HCl. SEM images of the nanoparticles shown in panel D after post-synthetic etching for 16 h in etching solutions containing 100 mM CTAC and 10 mM HCl (E) in the presence of 50 μM AgNO_3 and (F) in the absence of AgNO_3 . All SEM images share the same scale bar in panel A. In all these experiments, the preformed nanoparticles were first separated from their growth solution through centrifugation, then washed with water through redispersion and centrifugation, and finally redispersed in the etching solutions.

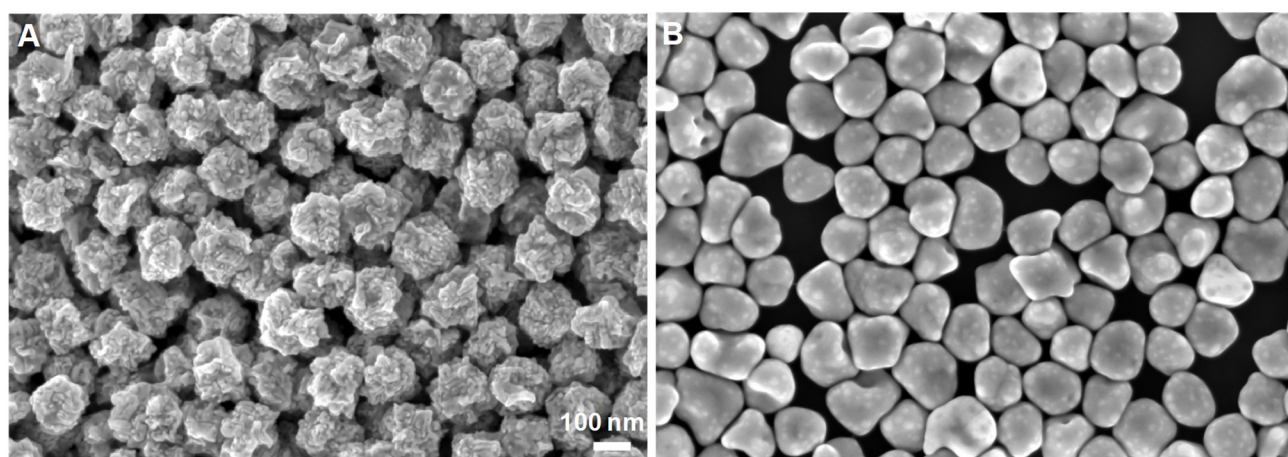


Figure S14. (A) SEM image of Au nanoparticles synthesized after 16 h in a growth solution containing 100 mM CTAC, 500 μM HAuCl_4 , and 1.2 mM AA. (B) SEM image of the nanoparticles obtained after exposing the nanoparticles shown in panel A to an etching solution containing 100 mM CTAC and 10 mM HCl for 16 h. Both SEM images share the same scale bar in panel A.

S4. References for Electronic Supplementary Information

1. M. L. Personick, M. R. Langille, J. Zhang and C. A. Mirkin, *Nano Lett.*, 2011, **11**, 3394-3398.
2. J. Zhang, M. R. Langille, M. L. Personick, K. Zhang, S. Li and C. A. Mirkin, *J. Am. Chem. Soc.*, 2010, **132**, 14012-14014.
3. Q. F. Zhang, N. Large and H. Wang, *ACS Appl. Mater. Interfaces*, 2014, **6**, 17255-17267.
4. Q. F. Zhang, H. Jing, G. G. Li, Y. Lin, D. A. Blom and H. Wang, *Chem. Mater.*, 2016, **28**, 2728-2741.
5. Q. F. Zhang, N. Large, P. Nordlander and H. Wang, *J. Phys. Chem. Lett.*, 2014, **5**, 370-374.
6. J. E. Millstone, S. Park, K. L. Shuford, L. D. Qin, G. C. Schatz and C. A. Mirkin, *J. Am. Chem. Soc.*, 2005, **127**, 5312-5313.
7. H. Wei, A. Reyes-Coronado, P. Nordlander, J. Aizpurua and H. X. Xu, *ACS Nano*, 2010, **4**, 2649-2654.
8. H. Wang and N. J. Halas, *Adv. Mater.*, 2008, **20**, 820-825.
9. A. S. Kumbhar, M. K. Kinnan and G. Chumanov, *J. Am. Chem. Soc.*, 2005, **127**, 12444-12445.